EMPLOYING LI-RADS ON DYNAMIC MRI SCANS FOR DISTINGUISHING HEPATOCELLULAR CARCINOMA FROM OTHER HEPATIC FOCAL LESIONS IN HIGH RISK PATIENTS

Heba Said Ellaban*, Rasha Abdelhafiz Aly* and Sameh Abokoura*.

***** Department of radiology - National Liver Institute, Menoufia University, Menoufia, Egypt.

Corresponding author:

Heba Said Ellaban
Mobile: +02 01155343799

Email:

hobasaidsaid@gmail.com,
Received: 13/5/2023
Accepted: 18/6/2023

Online ISSN: 2735-3540

ABSTRACT:

Background: *LI-RADS (Liver Imaging Reporting and Data System) provide standardization for screening high risk patients for hepatocellular carcinoma (HCC). Moreover, it aids in treatment response assessment. HCC is special among different malignancies in having tumor hallmark on dynamic CT or MRI that permit accurate diagnosis without an invasive biopsy.*

Objective: *To appraise LI-RADS on dynamic MRI scans for distinguishing hepatocellular carcinoma from other hepatic focal lesions in high risk patients.*

Patients and methods: *This study was designed in a retrospective pattern. It included eighty five high risk patients for hepatocellular carcinoma who had undergone dynamic MRI scans. Dynamic MRI scans were evaluated using LI-RADS features for distinguishing hepatocellular carcinoma from other hepatic focal lesions. Eventually, the obtained results were correlated with serial imaging follow-up or histopathological diagnosis as the diagnostic standard of reference.*

Results: *The majority of the included patients were found to have malignant lesions (67.1%) predominantly HCC (45.9%), followed by cholangiocarcinoma (8.2%) and finally hepatic deposits (7.1%). Considering LI-RADS categorization, hemangioma was most common among LIRAD1 group (60%), regeneration nodule among LIRAD 2 group (88.9%), dysplastic nodule among both LIRAD3 (50%) and LIRAD 4 groups (55.6). HCC among LIRAD5 group (100%). Finally, cholangiocarcinoma among LRM group (53.8 %).*

Conclusions: *Employing LI-RADS on dynamic MRI scans for distinguishing hepatocellular carcinoma from other hepatic focal lesions in high risk patients improves patient management*

Keywords: *Hepatic focal lesions, HCC, LI-RADS, Magnetic resonance imaging, Benign, Malignant*

INTRODUCTION:

Hepatocellular carcinoma (HCC) is one of the most frequent tumors universally[1]. Liver cirrhosis particularly is the main risk factor for HCC development, in patients with chronic viral infection (hepatitis B and C) and excess alcohol intake[2-4].

HCC is characterized by unique tumor features on magnetic resonance imaging (MRI) or multislice contrast-enhanced computed tomography (CT) that allow for accurate HCC diagnosis without an invasive procedure for confirmation[5, 6].

For HCC diagnosis, the dynamic imaging studies depend mainly on distinguishing the enhancement pattern of a suspected tumor relative to the hepatic background in the three hepatic phases (arterial, porto-venous and delayed)[7]. The

differences in vascular flow between HCC tissues and surrounding non-neoplastic hepatic tissue lead to distinctive imaging features during the dynamic post-contrast study, including arterial phase hyper-enhancement, washout pattern and finally, enhanced capsule[8]**.**

Over the years, managing HCC has followed various methods that depend on several morphologic features related to tumor (as number, size and vascular invasion) and clinical characteristics. However, these processes are improbable to recap the entire aspect of aggressive tumor with perfect prognosis[9].

The Liver Imaging Reporting and Data System, (LI-RADS) provides categorization for HCC imaging in the screening backgrounds of diagnosis and also, assessment of treatment response[10]. LI-RADS category was initiated by an association of radiologists as well as different specialists with high experience in imaging of hepatic cancer and it was involved into the latest HCC clinical practice management to assess the probability of HCC and overall malignancy[11].

The high risk group aimed by LI-RADS category involves patients with current or prior HCC following liver cirrhosis, chronic hepatitis B virus infection, along with living donor hepatic transplant recipients. LI-RADS do not be applicable to patients with vascular hepatic disorders or children. MRI examination is optimal for surveillance using LI-RADS because it has various contrast enhancement patterns and considered to be the single imaging tool that permits assessment of all major besides ancillary imaging features[12].

AIM OF THE STUDY:

The current study aimed to appraise LI-RADS on dynamic MRI scans for distinguishing hepatocellular carcinoma from other hepatic focal lesions in high risk patients

Ethics Approval and Consent to Participate:

All procedures followed were in accordance with the ethical standards of the responsible committee on human experimentation (Institutional Review Board (IRB)" of National Liver Institute Menoufia University and with the Helsinki Declaration of 1964 and later versions. Committee's reference number is (00355/2022). No consent was obtained from the patients since it was a retrospective study.

PATIENTS AND METHODS:

Patients:

We retrospectively included eighty five high risk patients for HCC from our institutional data base between May 2021 and June 2022. We included patients who were subjected to complete history taking, full clinical assessment and dynamic MRI scans for evaluation of hepatic focal lesions. Dynamic MRI scans were then evaluated using LI-RADS features for distinguishing hepatocellular carcinoma from other hepatic focal lesions. Eventually, the obtained results were correlated with serial imaging follow-up or histopathological diagnosis as the diagnostic standard of reference. The Ethical Committee approved our study protocol.

The exclusion criteria were lack of clinical database, age below 18 years and incomplete serial imaging follow-up or histopathological diagnosis.

MR imaging:

All MR examinations were performed at a 1.5 Tesla MR scanner (GE, 32 channels), using a phased-array body coil. Patients were asked to fast for 8 h prior to the study. The protocol imaging included precontrast and postcontrast (dynamic) studies. Precontrast parameters included *T1-weighted (T1W) images*: repetition time (TR)=10 ms, echo time (TE) = 4.58 ms,

matrix 179/320, slice thickness 7-8 mm, slice gap 1–2 mm, and FOV=355 mm. *T2-weighted (T2W) images*: TR ≥ 445 ms, TE = 26–28 ms, matrix 180–200 × 240 with a field of view=365, slice thickness 7–8 mm, slice gap 1–2 mm. *T2 In-phase and out-phase gradient echo sequence*: TR=75–100 ms, TE=4.6 ms for in phase and 2.3 ms for out phase, matrix 143 × 240 with a field of view=345, slice thickness 7–8 mm, slice gap 0 mm. *fat suppression sequence*: TR ≥ 400 ms, TE = 80 ms, matrix 204 × 384 with a field of view = 365, slice thickness 7–8 mm, slice gap 1–2 mm. Dynamic study was completed after a injecting of 0.1 mmol/kg body weight of Gd-DTPA with a 2 ml/s rate, which was flushed with 20 ml of sterile saline. Dynamic imaging using the T1 technique was performed in the triphasic strategy, involving three phases [arterial phase (16–20 sec), porto-venous phase (45–60 sec), and delayed phase (3–5 min)] after contrast administration.

Image analysis:

The concerned lesion was analyzed by its morphological features including size, border, signal intensities, enhancing pattern in the dynamic imaging, in addition to the overall number and segment of the detected focal lesions. The concerned MRI parameters included diffusion-weighted imaging (DWI) signal, T2 signal intensity, blood in the lesion, corona enhancement, mosaic architecture, enhancing capsule, iron in the lesion, nodule in a nodule appearance, fat content and blood pool enhancement. Eventually, the obtained results were correlated with serial imaging follow-up or histopathological diagnosis as the diagnostic standard of reference.

The ancillary features favoring benignity as marked T2 hyperintensity and blood pool enhancement. On the other hand, the ancillary features favoring malignancy, but not particularly HCC, as mild to moderate T2WI hyperintensity, DWI restriction, corona enhancement, capsule enhancement and blood within the lesion. While, the ancillary features favoring particularly HCC, as intra-tumoral fat, mosaic architecture and nodule-in-nodule architecture.

Statistical analysis:

IBM SPSS software package version 20.0 (Armonk, NY: IBM Corp) was used. Quantitative data were presented as numbers and percentages, whereas, quantitative data were presented as range (minimum and maximum), standard deviation, mean, and median. Sensitivity, specificity, and accuracy for agreement between malignancy and MRI parameters were used by Receiver operating characteristic curve analysis (ROC curve). P value ≤0.5 considered a significance level.

Our study limitations were a single center research, the small sample size and some bias in-patient selection.

RESULTS:

In this cohort study, eighty five patients with eighty five hepatic focal lesions were assessed by dynamic MRI scans since the main focal lesion was considered for the analysis if the patient had more than one lesion. Most of included patients were males (72.9%) with mean of age (59.3 ± 13.5) and size of the lesions (3.68 ± 2.24). The majority of patients were found to have malignant lesions (67.1%) with predominant HCC (45.9%) **(Figures 4,6),** followed by cholangiocarcinoma (8.2%) **(Figure 5)** and finally hepatic deposits (7.1%). From the entire 39 HCC cases, 35 out of them (89.7%) were correctly classified as HCC definitely diagnosed HCC (LR-5) and 4 tumors (10.3%)-probably HCC (LR-4). None of them was incorrectly diagnosed as benign (LIRAD1) or undifferentiated as LR-M.

Regarding the benign lesions, 23 patients were diagnosed (27.1%): 14 regenerative hepatic nodules (16.5%), 9

hepatic hemangiomas (10**.6%) (Figure 8)** and finally, focal nodular hyperplasia-FNH (Figure 7), confluent hepatic fibrosis and biliary cyst adenoma with each representing one patient (1.2 %) **(Table1).** The final diagnosis and the types of hepatic lesions according to

LI-RADS category was listed in Table 2. Hemangioma was the most common among LIRAD1 group (60%), regeneration nodule among LI-RAD 2 group (88.9%), dysplastic nodule among both LI-RAD3 (50%) and LI-RAD 4 groups (55.6). HCC among LI-RAD5 group (100%). Finally, cholangiocarcinoma among LRM group (53.8 %).

Analysis of our cases showed that ancillary features favoring malignancy in general at MRI to discriminate malignant included the following; DWI signal with restricted diffusion with a sensitivity 91.23 and specificity of 89.29, mosaic architecture had sensitivity 84.21 and specificity of 100, nodule in a nodule appearance had sensitivity 75.44 and specificity of 100 and so on **(Tables 3-5).**

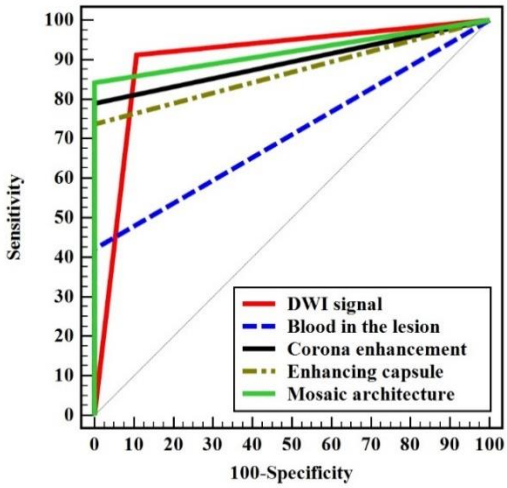

Figure (1): ROC curve for ancillary features favoring malignancy in general at MRI to discriminate Malignant (n = 57) from Benign (n = 28)

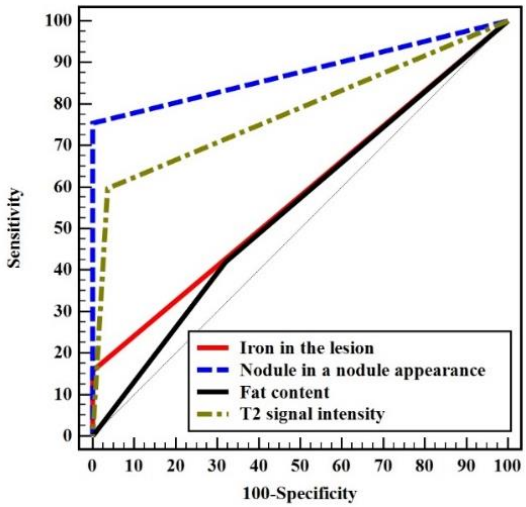

Figure (2): ROC curve for ancillary features favoring malignancy in general at MRI to discriminate Malignant (n = 57) from Benign (n = 28).

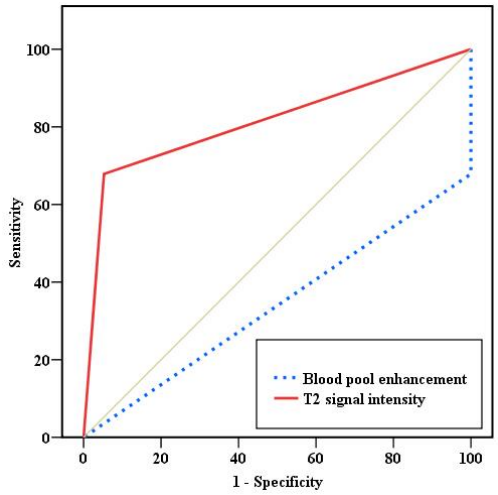

Figure (3): ROC curve for ancillary features favoring benignity at MRI to discriminate Benign (n = 28) from Not benign (n = 57)

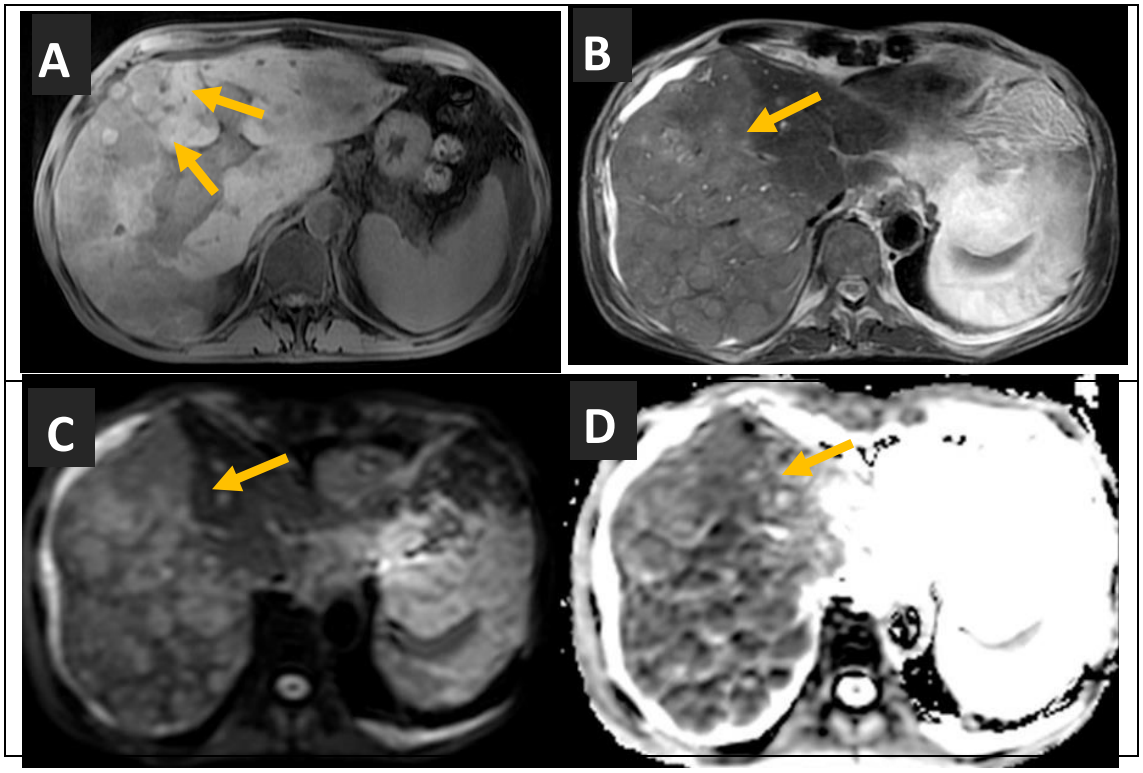

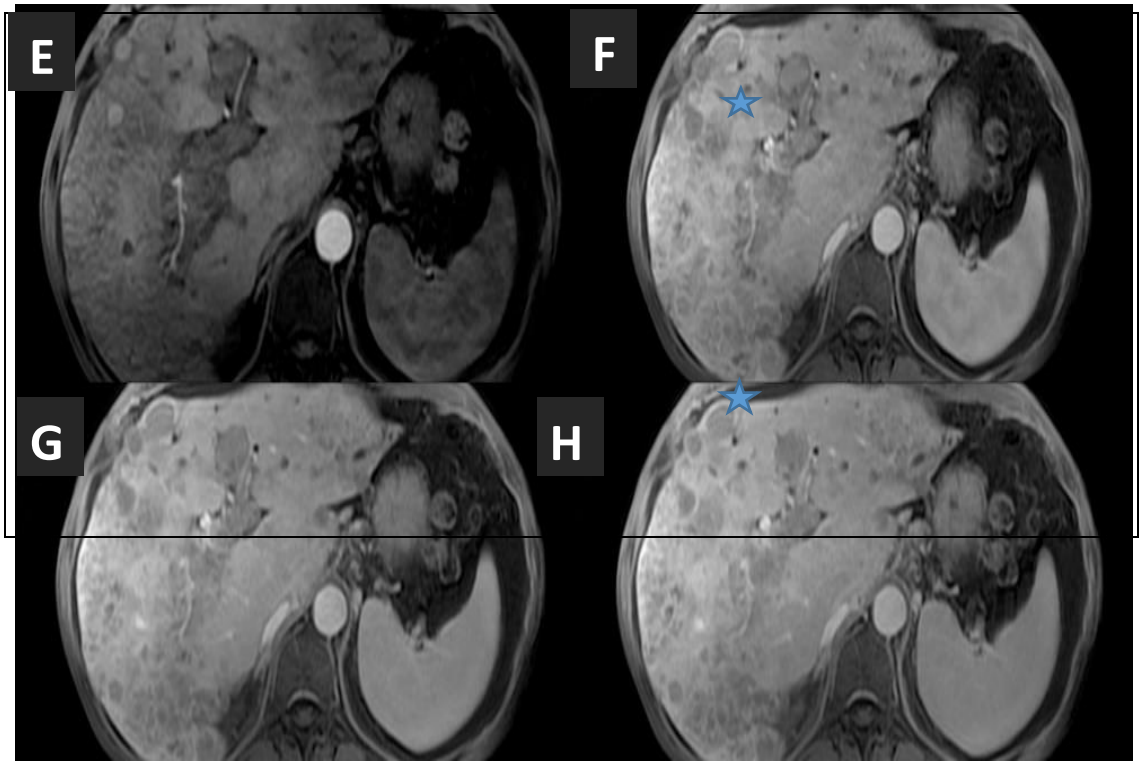

Figure (4): A 70-year old male patient with right hepatic lobe infiltrative HCC with internal hemorrhagic foci invading the left, right and main portal veins with left hepatic lobe satellite lesions (LI-RAD5), the diagnostic standard of reference serial imaging follow-up. A: Axial non-contrast T1WI shows hyperintense foci of hemorrhage (arrows) within the lesion. B: Axial T2WI shows mild high signal intensity of the lesion (arrow), perihepatic ascites. C, D: Axial DWI and ADC images show restricted diffusion of the lesion. E, F: Axial arterial and delayed arterial phases images (star) show faint arterial enhancement of the infiltrative right hepatic lobe lesion. G, H: Axial porto-venous and delayed phases images (blue star) show faint contrast wash out of the lesion.

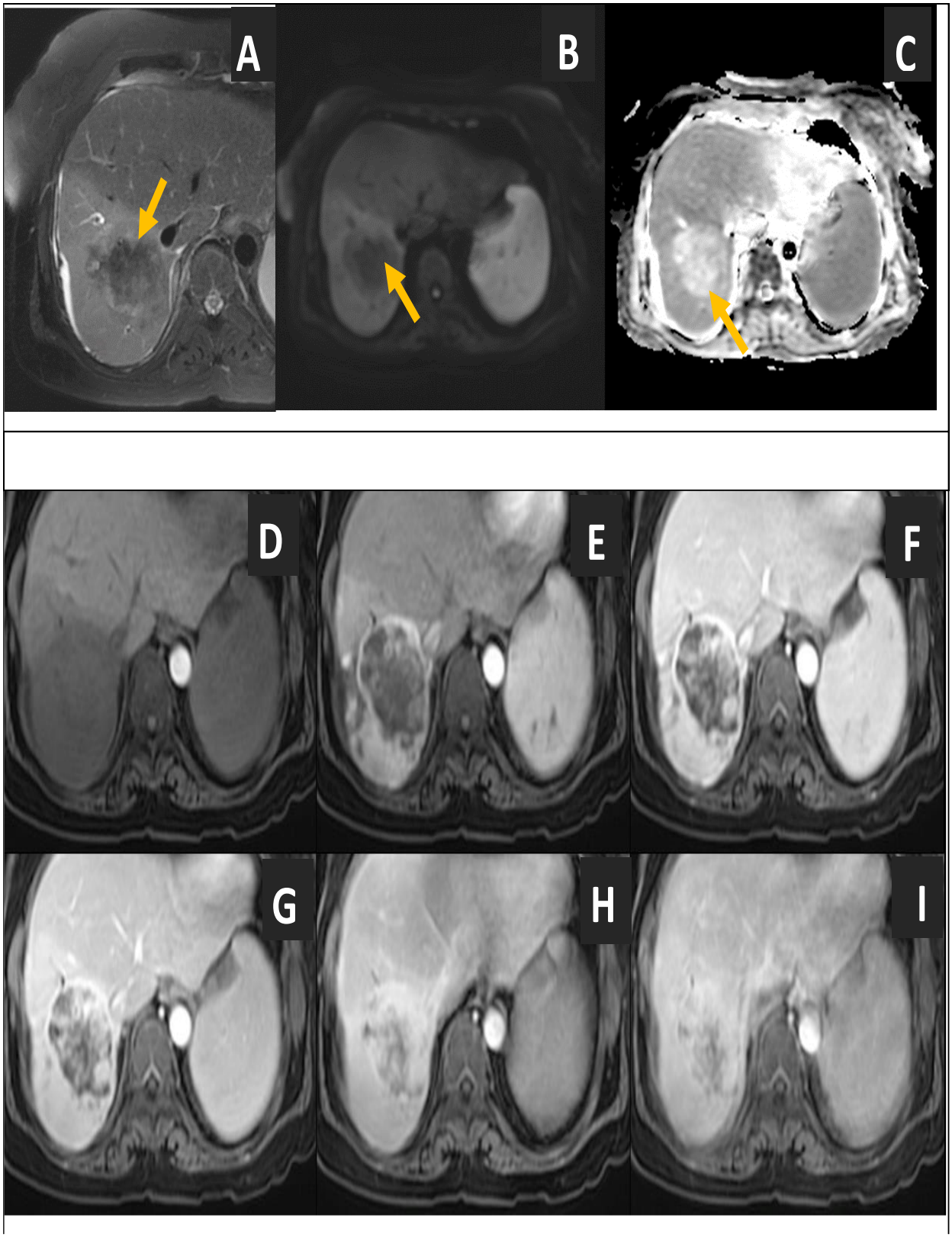

Figure (5): A 55-years old female patient with right hepatic lobe segment VII cholangiocarcinoma on top of liver cirrhosis (LI-RAD M), the diagnostic standard of reference serial imaging follow-up and enhancement pattern. A: Axial T2WI image shows central hypointense signal intensity of the lesion with peripheral mild hyperintensity, minimal perihepatic ascites. B, C: Axial DWI and ADC images

(arrow) show no restricted diffusion of the lesion. D to I: Axial dynamic study images show arterial peripheral inhomogeneous enhancement with filling in pattern on the sequential phases.

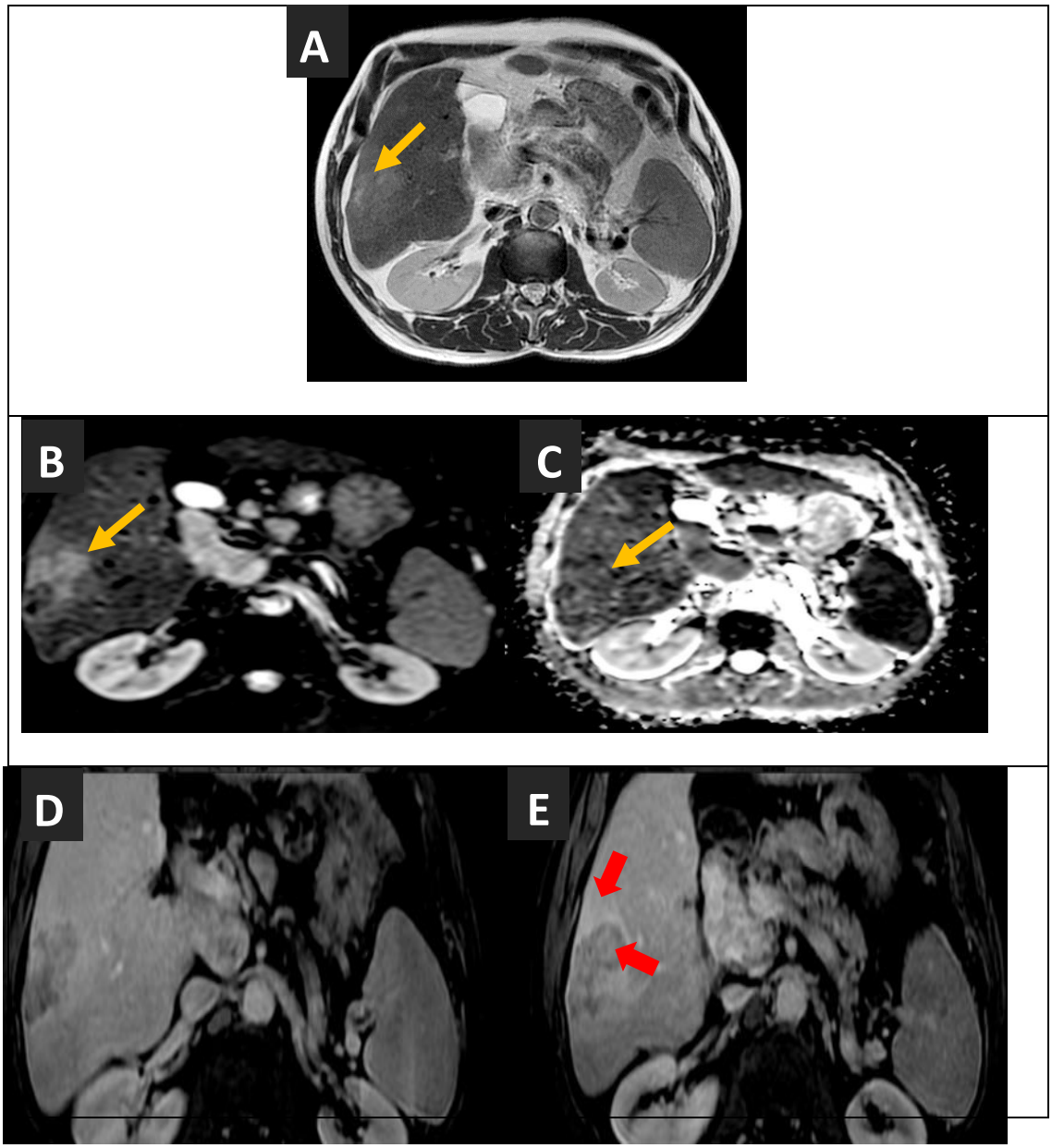

Figure (6): A 65-year old male patient with right hepatic lobe segment VI HCC on top of liver cirrhosis (LI-RAD 5), the diagnostic standard of reference serial imaging follow-up. A: Axial T2WI image shows mild to moderate hyperintense signal intensity of the lesion *(arrow)*. B, C: Axial DWI and ADC images show mild restricted diffusion of the lesion *(arrows)*. D, E: Axial post-contrast enhanced images show corona enhancement of the lesion *(red arrows)*.

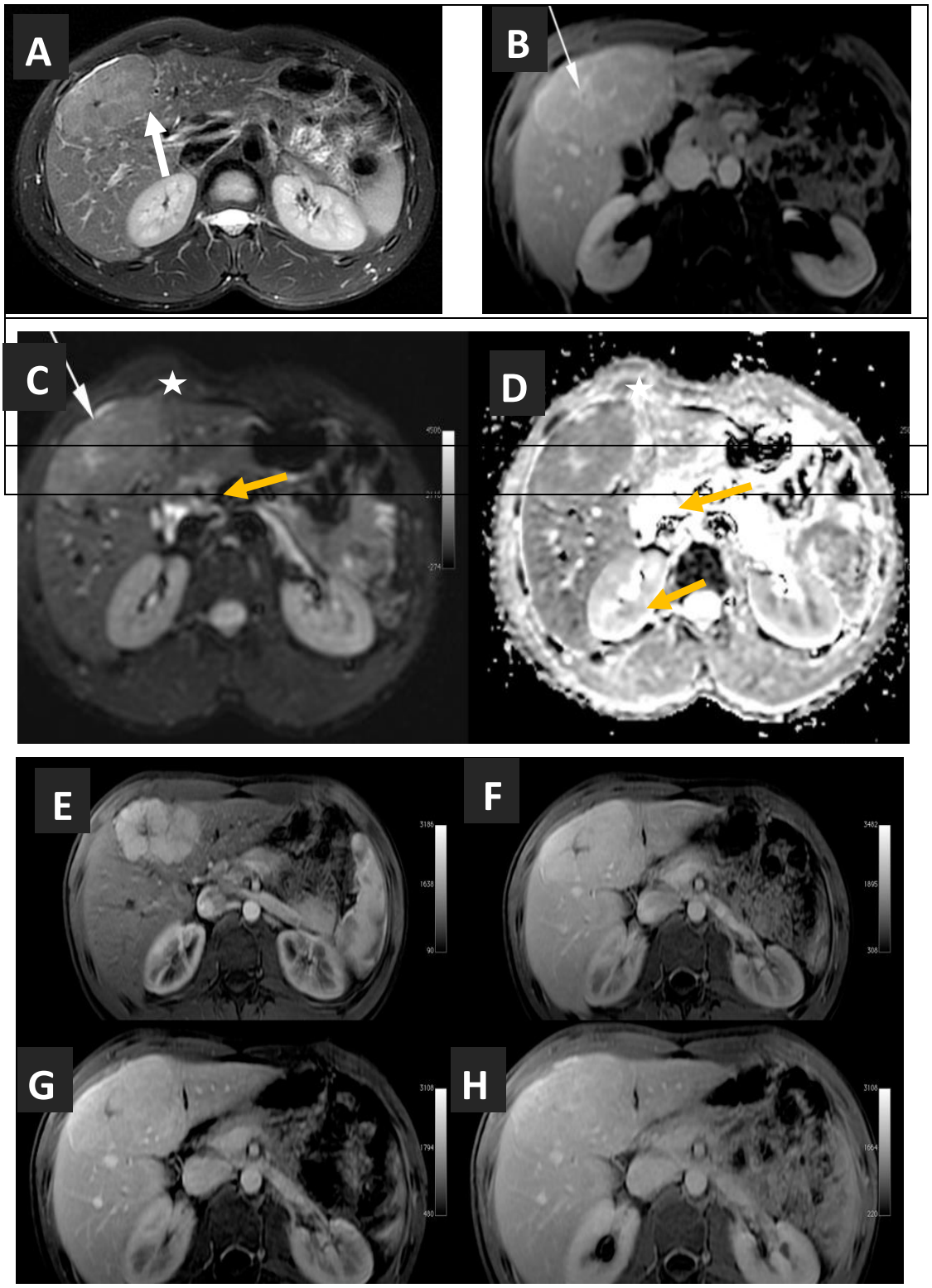

Figure (7): A 44-year old male patient with chronic hepatitis C with segment IV focal nodular hyperplasia (LI-RAD2), the diagnostic standard of reference is biopsy A: Axial T2WI image shows segment IV lesion *(orange arrow)* with mild high signal intensity with central hypointense scar *(white arrow)*. B: Axial delayed phase image shows a delayed enhancing central scar *(thin white arrow)*. C, D: Axial DWI and ADC images show free diffusion of the lesion *(white star)*. E: Axial early arterial phase image shows intense arterial enhancement of the lesion. F, G, H: Axial delayed arterial, porto-

venous and delayed phases images show that the lesion becomes isointense to the liver *(orange arrow).*

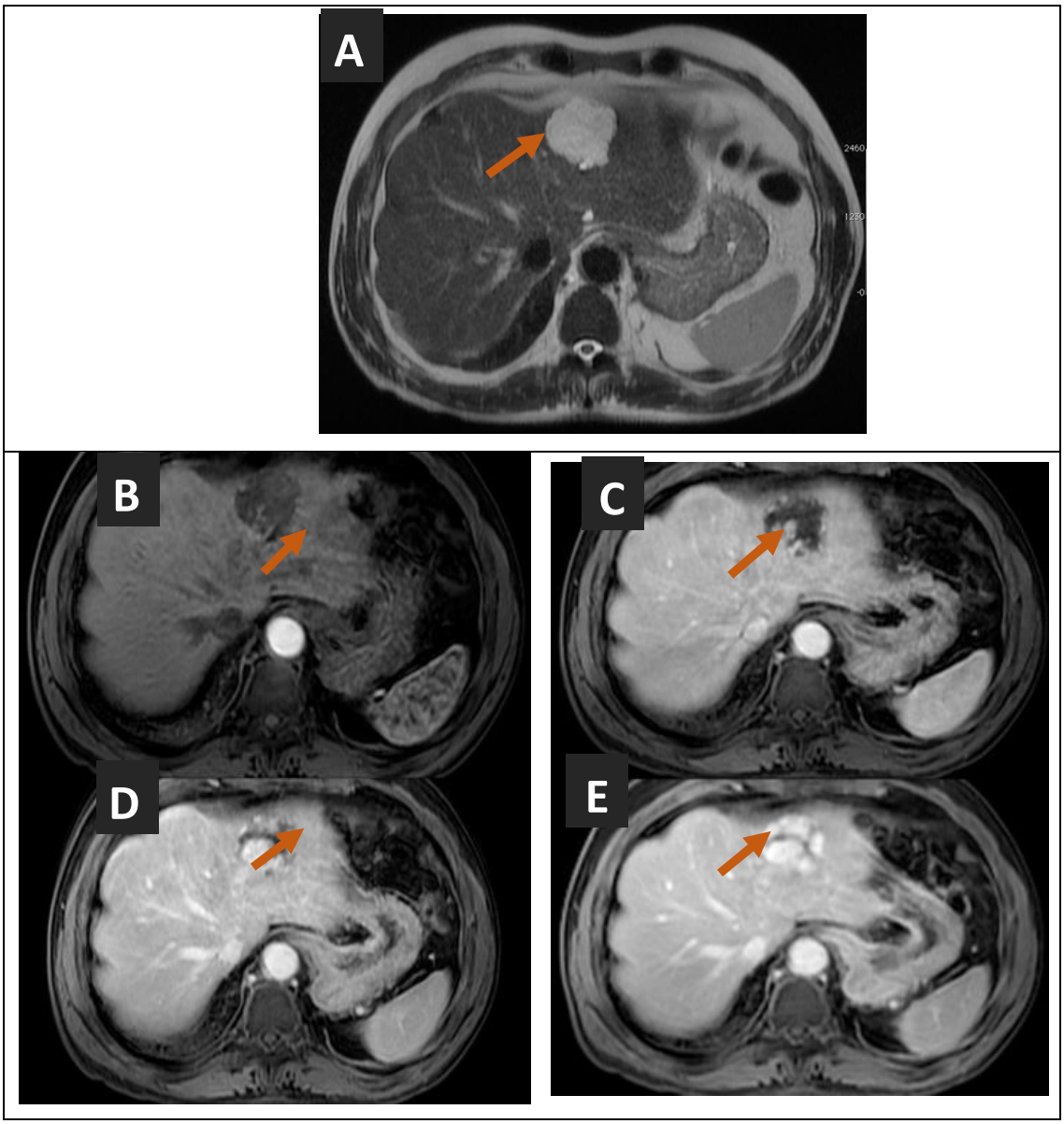

Figure (8): A 55-year old female patient with chronic hepatitis B, presented with segment II hemangioma (LI-RAD2),the diagnostic standard of reference is biopsy. A: Axial T2WI image shows segment II lesion with lobulated surface and marked high signal intensity *(arrow).* B, C: Axial early and delayed arterial phase images show peripheral nodular enhancement of the lesion *(arrow).* D, E: Axial porto-venous and delayed phase images show centripetal filling in pattern *(arrow).*

Table (1): Distribution of the studied hepatic focal lesions according to different parameters (n = 85).

	No. (%)
Sex	
Male	62 (72.9%)
Female	23 (27.1%)
Age (/years)	
Mean ± SD.	59.3 ± 13.5
Median (Min. – Max.)	56 (25 – 88)
Malignancy	
Benign	28 (32.9%)
Malignant	57 (67.1%)
Focal lesion	
Hemangioma	9 (10.6%)
Regeneration nodule	14 (16.5%)
Dysplastic nodule	7 (8.2%)
Focal nodular hyperplasia	1 (1.2%)
Confluent hepatic fibrosis	1 (1.2%)
Biliary cyst adenoma	1 (1.2%)
Cholangiocarcinoma	7 (8.2%)
Hepatic deposits	6 (7.1%)
HCC	39 (45.9%)
LI-RAD	
LI-RAD1	15 (17.6%)
LI-RAD2	9 (10.6%)
LI-RAD3	4 (4.7%)
LI-RAD 4	9 (10.6%)
LI-RAD 5	35 (41.2%)
LRM	13 (15.3%)
Size of the lesions (cm)	
Mean ± SD.	3.68 ± 2.24
Median (Min. – Max.)	3.5 (0.5 – 9)
DWI signal	
Low	30 (35.3%)
High	55 (64.7%)
T2 signal intensity	
Low	6 (7.1%)
Mild high	12 (14.1%)
Mild to moderate high	35 (41.2%)
Moderate high	10 (11.8%)
Marked high	22 (25.9%)
Blood in the lesion	24 (28.2%)
Corona enhancement	45 (52.9%)
Enhancing capsule	42 (49.4%)
Mosaic architecture	48 (56.5%)
Iron in the lesion	9 (10.6%)
Nodule in a nodule appearance	43 (50.6%)
Fat content	33 (38.8%)
Blood pool enhancement	9 (10.6%)

SD: Standard deviation

Table (2): Distribution of the studied hepatic focal lesions according to LI-RADS in each cases type

	Total	LI-RAD1	LI-RAD2	LI-RAD3	LI-RAD4	LI-RAD 5	LRM
Cases							
Hemangioma	9 (10.6%)	9 (60%)	0 (0%)	0 (0%)	0 (0%)	0 (0%)	0 (0%)
Regeneration nodule	14(16.5%)	6 (40%)	8 (88.9%)	0 (0%)	0 (0%)	0 (0%)	0 (0%)
Dysplastic nodule	7 (8.2%)	0 (0%)	0 (0%)	2 (50%)	5 (55.6%)	0 (0%)	0 (0%)
Focal nodular hyperplasia	1 (1.2%)	0 (0%)	1 (11.1%)	0 (0%)	0 (0%)	0 (0%)	0 (0%)
Confluent hepatic fibrosis	1 (1.2%)	0 (0%)	0 (0%)	1 (25%)	0 (0%)	0 (0%)	0 (0%)
Biliary cyst adenoma	1 (1.2%)	0 (0%)	0 (0%)	1 (25%)	0 (0%)	0 (0%)	0 (0%)
Cholangiocarcinoma	7 (8.2%)	0 (0%)	0 (0%)	0 (0%)	0 (0%)	0 (0%)	7 (53.8%)
Hepatic deposits	6 (7.1%)	0 (0%)	0 (0%)	0 (0%)	0 (0%)	0 (0%)	6 (46.2%)
HCC	39 (45.9%)	0 (0%)	0 (0%)	0 (0%)	4 (44.4%)	35 (100%)	0 (0%)
Total	85 (100%)	15 (100%)	9 (100%)	4 (100%)	9 (100%)	35 (100%)	13 (100%)

Table (3): ROC curve for ancillary features favoring malignancy in general at MRI to discriminate Malignant (n = 57) from Benign (n = 28)

		Malignancy		Sensitivity	Specificity	PPV	NPV	Accuracy	AUC	p	95% C. I
		Benign (n=28)	Malignant (n=57)								
DWI signal	Free diffusion	25	5	91.23	89.29	94.55	83.33	90.59	0.903	<0.001*	0.824-0.982
	Restricted	3	52								
Blood in the lesion	No	28	33	42.1	100.0	100.0	45.9	61.2	0.711	0.002*	0.604-0.817
	Yes	0	24								
Corona enhancement	No	28	12	78.95	100.0	100.0	70.0	85.88	0.895	<0.001*	0.827-0.962
	Yes	0	45								
Enhancing capsule	No	28	15	73.68	100.0	100.0	65.12	82.35	0.868	<0.001*	0.793-0.943
	Yes	0	42								
Mosaic architecture	No	28	9	84.21	100.0	100.0	75.68	89.41	0.921	<0.001*	0.862-0.980
	Yes	0	48								

PPV: Positive predictive value, NPV: Negative predictive value, AUC: Area under a Curve, p value: Probability value, CI: Confidence Intervals, *: Statistically significant at $p \leq 0.05$.

Table (4): ROC curve for ancillary features favoring malignancy in general at MRI to discriminate Malignant (n=57) from Benign (n=28)

		Malignancy		Sensitivity	Specificity	PPV	NPV	Accuracy	AUC	p	95% C.I
		Benign (n = 28)	Malignant (n = 57)								
Iron in the lesion	No	28	48	15.8	100.0	100.0	36.8	43.5	0.579	0.239	0.455-0.703
	Yes	0	9								
Nodule in a nodule appearance	No	28	14	75.44	100.0	100.0	66.67	83.53	0.877	<0.001*	0.805-0.950
	Yes	0	43								
Fat content	No	19	33	42.1	67.9	72.7	36.5	50.6	0.550	0.457	0.420-0.679
	Yes	9	24								
T2 signal intensity	Others	27	23	59.65	96.43	97.14	54.0	71.76	0.780	<0.001*	0.683-0.877
	Mild to moderate high	1	34								

Table (5): ROC curve for ancillary features favoring malignancy in general at MRI to discriminate Malignant (n = 57) from Benign (n = 28).

		Malignancy		Sensitivity	Specificity	PPV	NPV	Accuracy	AUC	p	95% CI
		Not benign (n = 57)	Benign (n = 28)								
Blood pool enhancement		0 57	9 19	100.0	32.14	75.0	100.0	77.65	0.339	0.016*	0.205-0.473
T2 signal intensity	Others	54	9	67.86	94.74	86.36	85.71	85.88	0.813	<0.001*	0.701-0.925
	Marked high	3	19								

PPV: Positive predictive value, **NPV:** Negative predictive value, **AUC:** Area under a Curve, **p value:** Probability value, **CI:** Confidence Intervals, *: Statistically significant at $p \leq 0.05$

DISCUSSION:

Initial diagnosis is an essential strategy in HCC patient's management. Contrast-enhanced MRI can provide a full wealth data with regarding tumor hemodynamics, morphology, and function. The specific enhancement pattern that is characterized by contrast uptake in arterial phase and washout in the venous and delayed phases providing the HCC's diagnostic criteria. The remarkable sign has 100% specificity when revealed on dynamic contrast MR study in high-risk patients for HCC [9&13]**.** The characteristic vascular manner is related to intramodular hemodynamic changes all through carcinogenesis process and to appreciate the HCC hemodynamics is crucial for the proper analysis, as there is a profound association between their hemodynamics and pathophysiological theories [14&15]**.**

Actually, LIRADS expresses three groups of hepatic focal lesion with probability of HCC: definite benign nodules (LR-1) (17.6%), intermediate HCC probability (LR-2) (10.6%), (LR-3) (4.7%) and (LR-4) (10.6%) and definitive HCC diagnosis (LR-5) (41.2%). Grey zone ranges from 20% to 80%. In a lately published review, *Van der Pol et al.,*[16] showed that the probability of HCC for LR-2, LR-3, LR-4, LR-5 and LR-M groups was: 13% (CI 18–22), 38% (CI 31–45), 74% (CI 67–80), 94% (CI 92–96) and 36% (CI 26–48), respectively. Also, *Park et al.,*[17] found that confidence intervals (CI) showed intermediate possibility have a wide scale of HCC likelihood. In another study HCC probability for LR-3 to LR-5 categories was 47%, 85% and 98%, respectively using contrast-enhanced ultrasound[18]**.**

The current study showed that high DWI signal was the best method for MRI ancillary features favoring malignancy in general to discriminate malignant with sensitivity of 91.23, specificity of 89.29. Some studies by **Inchingolo et al.,**[19] **and Piana et al.,**[20] supported the use of diffusion weighted imaging (DWI) in diagnosing HCC, particularly in association with hypointensity on the dynamic post-contrast study. At the same time, others documented only moderate or no added value of DWI in conventional MR imaging, as some HCCs may show no or minimal restricted diffusion. [21] Also, **De Gaetano et al.,**[22] found that sensitivity and specificity of restricted diffusion were respectively of 58.8% and 65.4% for the diagnosis of HCC, much lower than previous values. **Basha et al.,**[23] supported the use of diffusion weighted imaging (DWI) in diagnosing

HCC in combination with ADC value on ADC map which increased the sensitivity of HCC diagnosis.

Lesional hyper-enhancement in arterial phase is an important pre-requisite for HCC (LR-5), but it is non-specific. Indeed, regarding the hepatocarcinogenesis this feature may be not present, so as it may be also seen in benign entities like dysplastic nodules and arterio portal shunts[24]**.** Similarly to our study as lesional hyper enhancement had sensitivity of 87.7, specificity of 32.1.They confirmed that there is high specificity of lesion washout dynamic contrast in contact with informed values ranging from 62% to 95% and confirmed that the arterial phase hyperenhancement combination with washout a criterion usually used in diagnostic systems[25&26]**.**

Holland et al.,[27] revealed that in proven cases with HCC, the majority of arterial phase hypervascular lesions on that were not identified on T2 WI and portal phase after contrast administration was non-malignant in nature. On the contrary, ***Kim et al.*,[28]** confirmed that, the most important findings related to HCC, in lesions less than 2 cm, were arterial phase hyperenhance-ment. *Ehman et al.,***[29]** proved that arterial hyperenhancement was the most detected criterion in most of diagnosed HCC and was seen somewhat more commonly at CT examination versus MRI (87 vs. 86%). Conversely, ***Burrel et al.,***[30] exhibited that sensitivity of MR was better than CT in HCC detection (76% vs 61%).

Regarding other ancillary features favoring malignancy in general at MRI included the following; enhancing capsule with a sensitivity of 73.68 and specificity of 100, In this concern, **De Gaetano et al.,**[22] enhancing "capsule" showed a high specificity of 88.5% for HCC. This feature was significantly correlated to the histological classification of nodules and was most frequently observed in HCCs.

Corona enhancement is seen as an enhancement in the peritumoral parenchyma and considered as a feature of hypervascular HCC. It begins a few seconds after lesion enhancement, so that with apparent larger tumor size, tumor and corona enhancement may overlap. Its presence aids to distinguish highly vascular HCCs from pseudo-lesions; however it is not a marker of HCC.**[31].** Regarding our study corona enhancement had sensitivity of 78.95 and specificity of 100, this was in line with **Ju et al.,[32]** revealed that , the overall incidence of corona enhancement was the highest among small HCCs on contrast enhanced MRI as well as corona enhancement could be more sensitive than enhancing.

Mosaic architecture states to the presence of intralesional difference in intensity and enhancement, likely with intervening fibrous septa. In our study mosaic architecture with a sensitivity of 84.21 and specificity of 100, this feature is mainly seen in large size HCCs and reveals the mosaic appearance at histopathologic assessment. **Choi et al.,[31]** revealed that the previous feature is unfamiliar in tumors other than HCC.

Lesional iron raises concern for pre-malignant or malignant nodules. However, it is not particular for high-grade HCC, but this appearance has been seen in other non-HCC malignancies. **[31]** this is in line with our study as we found iron in the lesion signal had a sensitivity of 15.8, specificity of 100,

In our study mild-moderate T2 signal intensity had sensitivity 59.65, specificity of 96.43. *De Gaetano et al.,*[22] found that, mild-moderate T2 hyperintensity showed moderate sensitivity (64.7%) and specificity (61.5%) for HCC, similar to values of *Hecht et al.***[24].** Thus, although mild-moderate T2 hyperintensity did not significantly correlate to the histological classification of nodules, it was mostly encountered in HCCs, in agreement with the literature[9].

Furthermore, ***De Gaetano et al.,***[22] reported that, fat in a mass, more than in the adjacent hepatic parenchyma, was observed in 11.8% of HCCs, with a specificity of 76.9%. However, ***Rimola et al.,*** [35] encountered fat in mass was not significantly correlated to histological classification of HCC. The overall diagnostic performance hence is limited because fat in a mass, more than in the hepatic background, does not provide reliable difference of HCCs from other lesions [36]**.** All were in line with our study as fat content had sensitivity 42.1, specificity of 67.9 and

According to the recently released update of Liver Imaging and Reporting Data System (LI-RADs v2018), the nodule-in-nodule architecture is an ancillary feature favoring HCC in particular. When detected, it may be used to upgrade an observation by one LI-RADS category only, up to LR-4[37]**.** This was similarly to nodule in a nodule appearance in our study with sensitivity of 75.44, specificity of 100.

Regarding other ancillary features favoring benginity in general at MRI included the following blood pool enhancement pattern and T2 marked hyperintensity, our study reported blood pool enhancement pattern had sensitivity of 100and specificity of 32.1, T2 hyperintensity had sensitivity of 67.86and specificity of 94.74, these results were in line with **choi et al.,**[26] that reported that most of bengin lesion display high signal intensity on T2WI as well as blood pool enhancement is specific for benign lesions.

Our study limitations were a single center research, the small sample size and some bias in-patient selection.

Conclusions:

The LI-RADS yields a diagnostic guidance targeted at differentiating the hepatocellular carcinoma from other hepatic focal lesions, in a high-risk patient for to obtain perfect management.

Declarations

Consent for publication:

All patients included in this research gave written informed consent to publish the data contained within this study.

Availability of data and materials:

The datasets used and/or analyzed during the current study are available from the corresponding author on reasonable request.

Competing interests:

The authors declare that they have no competing interests.

Funding:

This study had no funding from any resource.

Authors' contributions: HSA: Conceptualization and Data curation: HS, Formal analysis: SA, HS, Investigation: HS Formal analysis: SA, HS, RA, Methodology: HS, Project administration and resources: SA, RA, Software: HS, Supervision: HS, Validation and Visualization: SA, HS, RA, **writing original draft:** HS, writing review, revised & editing: HS, RA, SA. "All authors read and approved the final manuscript".

Acknowledgements

Not applicable

List of abbreviation

LI-RADS: Liver Imaging Reporting and Data System, HCC: hepatocellular carcinoma, CT: enhanced computed tomography, MRI: magnetic resonance imaging, *T1W: T1-weighted*, *T2W: T2-weighted*, Ms: millisecond, mm: millimeter, TR: repetition time. TE: Time to Echo, Gd: gadolinium. AFs: ancillary features, CI: confidence intervals, FNH: focal nodular hyperplasia, sec: second

REFERENCES:

1. **Mittal S, El-Serag HB (**2013): Epidemiology of HCC: consider the population. Journal of clinical gastroenterology Jul; 47: S2.
2. **El-Serag HB** (2011): Current concepts. N Engl J Med; 365:1118-27.
3. **El-Serag HB (2012):** Epidemiology of viral hepatitis and hepatocellular carcinoma. Gastroenterology; May 1;142 (6):1264-73.
4. **Noureddin M, Rinella ME (2015):** Nonalcoholic fatty liver disease, diabetes, obesity, and hepatocellular carcinoma. Clinics in liver disease; May 1;19(2):361-79.
5. **Manini MA, Sangiovanni A, Fornari F, Piscaglia F, Biolato M, Fanigliulo L, Ravaldi E, Grieco A, Colombo M, Participants S** (2014): Clinical and economic impact of 2010 AASLD guidelines for the diagnosis of hepatocellular carcinoma. Journal of hepatology; May 1;60(5):995-1001.
6. **Sangiovanni A, Manini MA, Iavarone M, Romeo R, Forzenigo LV, Fraquelli M, Massironi S, Della Corte C, Ronchi G, Rumi MG, Biondetti P (**2010):The diagnostic and economic impact of contrast imaging techniques in the diagnosis of small hepatocellular carcinoma in cirrhosis. Gut; May 1;59(5):638-44.
7. **Yamashita Y, Mitsuzaki K, Yi T, Ogata I, Nishiharu T, Urata J, Takahashi** (1996): Small hepatocellular carcinoma in patients with chronic liver damage: prospective comparison of detection with dynamic MR imaging and helical CT of the whole liver. Radiology; Jul;200(1):79-84.
8. **Choi JY, Lee JM, Sirlin CB** (2014):CT and MR imaging diagnosis and staging of hepatocellular carcinoma: part I. Development, growth, and spread key pathologic and imaging aspects. Radiology; Sep;272(3):635.
9. **Wei H, Yang T, Chen J, Duan T, Jiang H, Song B** (2022): Prognostic implications of CT/MRI LI-RADS in hepatocellular carcinoma: State of the art and future directions. Liver International; Jul; 42:2131–2144.
10. **Marrero JA, Kulik LM, Sirlin CB, Zhu AX, Finn RS, Abecassis MM, Roberts LR, Heimbach JK** (2019): Diagnosis, staging, and management of hepatocellular carcinoma: 2018 practice guidance by the American Association for the Study of Liver Diseases. Clinical Liver Disease; Jan;13(1):1.
11. **Chernyak V, Fowler KJ, Kamaya A, Kielar AZ, Elsayes KM, Bashir MR, Kono Y, Do RK, Mitchell DG, Singal AG, Tang A** (2018): Liver Imaging Reporting and Data System (LI-RADS) version 2018: imaging of hepatocellular carcinoma in at-risk patients. Radiology; Dec;289(3):816.
12. **Cerny M, Chernyak V, Olivié D, Billiard JS, Murphy-Lavallée J, Kielar AZ, Elsayes KM, Bourque L, Hooker JC, Sirlin CB, Tang A** (2018): LI-RADS version 2018 ancillary features at MRI. Radiographics; Nov;38(7):1973-2001.
13. **An C, Rakhmonova G, Choi JY** (2016): Liver imaging reporting and data system (LI-RADS) version 2014: understanding and application of the diagnostic algorithm. Clin Mol Hepatol; 22(2):296–307.
14. **Centonze L, De Carlis R, Vella I** (2022): From LI-RADS classification to HCC pathology: a retrospective single-institution analysis of clinico-pathological features affecting oncological outcomes after curative surgery. Diagnostics (Basel);12(1):160
15. **Tang A, Bashir MR, Corwin MT, Cruite I, Dietrich CF, Do RK, Ehman EC, Fowler KJ, Hussain HK, Jha RC, Karam AR** (2018): Evidence supporting LI-RADS major features for CT-and MR imaging–based diagnosis of hepatocellular carcinoma: a systematic review. Radiology; Jan;286(1):29.
16. **Van der Pol CB, Lim CS, Sirlin CB, McGrath TA, Salameh JP, Bashir MR, Tang A, Singal AG, Costa AF, Fowler K, McInnes MD** (2019); Accuracy of the liver imaging reporting and data system in

computed tomography and magnetic resonance image analysis of hepatocellular carcinoma or overall malignancy—a systematic review. Gastroenterology; Mar 1;156(4):976-86.

17. **Park SH, Kim B, Kim SY, Shim YS, Kim JH, Huh J, Kim HJ, Kim KW, Lee SS** (2020): Abbreviated MRI with optional multiphasic CT as an alternative to full-sequence MRI: LI-RADS validation in a HCC-screening cohort. European Radiology; Apr;30(4):2302-11.
18. **Terzi E, Iavarone M, Pompili M, Veronese L, Cabibbo G, Fraquelli M** (2017): Contrast enhanced ultrasound identifies hepatocellular carcinoma in cirrhosis: a large multicenter retrospective study. J Hepatol; 10:32428-5.
19. **Inchingolo R, De Gaetano AM, Curione D, Ciresa M, Miele L, Pompili M, Vecchio FM, Giuliante F, Bonomo L** (2015): Role of diffusion-weighted imaging, apparent diffusion coefficient and correlation with hepatobiliary phase findings in the differentiation of hepatocellular carcinoma from dysplastic nodules in cirrhotic liver. European radiology; Apr;25(4):1087-96.
20. **Piana G, Trinquart L, Meskine N, Barrau V, Van Beers B, Vilgrain V** (2011): New MR imaging criteria with a diffusion-weighted sequence for the diagnosis of hepatocellular carcinoma in chronic liver diseases. Journal of hepatology; Jul 1;55(1):126-32.
21. **Izzo F, Albino V, Palaia R, Piccirillo M, Tatangelo F, Granata V, Petrillo A, Lastoria S** (2014): Hepatocellular carcinoma: preclinical data on a dual-lumen catheter kit for fibrin sealant infusion following loco-regional treatments. Infectious Agents and Cancer; Dec;9(1):1-6.
22. **De Gaetano AM, Catalano M, Pompili M, Marini MG, Gullì C, Infante A, Iezzi R, Ponziani FR, Cerrito L, Marrone G, Giuliante F** (2019): Critical analysis of major and ancillary features of LI-RADS v2018 in the differentiation of small (≤ 2 cm) hepatocellular carcinoma from dysplastic nodules with gadobenate dimeglumine-enhanced magnetic resonance imaging. European Review for Medical and Pharmacological Sciences; Sep 1;23(18):7786-801.
23. **Basha MAA, Refaat R, Mohammad FF, Khamis MEM, El-Maghraby AM, El Sammak AA et al** (2019): The utility of diffusion-weighted imaging in improving the sensitivity of LI-RADS classification of small hepatic observations suspected of malignancy. Abdominal Radiology;44:1773–84.
24. **Hecht EM, Holland AE, Israel GM, Hahn WY, Kim DC, West AB, Babb JS, Taouli B, Lee VS, Krinsky GA** (2006):Hepatocellular carcinoma in the cirrhotic liver: gadolinium-enhanced 3D T1-weighted MR imaging as a stand-alone sequence for diagnosis. Radiology; May;239(2):438-47.
25. **Lee KH, O'Malley ME, Haider MA, Hanbidge A** (2004): Triple-phase MDCT of hepatocellular carcinoma. American Journal of Roentgenology; Mar;182(3):643-9.
26. **Choi JY, Cho HC, Sun M, Kim HC, Sirlin CB** (2013): Indeterminate observations (liver imaging reporting and data system category 3) on MRI in the cirrhotic liver: fate and clinical implications. American Journal of Roentgenology; Nov; 201(5):993-1001.
27. **Holland AE, Hecht EM, Hahn WY, Kim DC, Babb JS, Lee VS, West AB, Krinsky GA** (2005): Importance of small (≤ 20-mm) enhancing lesions seen only during the hepatic arterial phase at MR imaging of the cirrhotic liver: evaluation and comparison with whole explanted liver. Radiology; Dec;237(3):938-44.
28. **Kim TK, Lee KH, Jang HJ, Haider MA, Jacks LM, Menezes RJ, Park SH, Yazdi L, Sherman M, Khalili K** (2011):Analysis of gadobenate dimeglumine–enhanced MR findings for characterizing small (1–2-cm) hepatic nodules in patients at high risk for hepatocellular carcinoma. Radiology; Jun;259(3):730-8.

29. **Ehman EC, Behr SC, Umetsu SE, Fidelman N, Yeh BM, Ferrell LD, Hope TA** (2016): Rate of observation and inter-observer agreement for LI-RADS major features at CT and MRI in 184 pathology proven hepatocellular carcinomas. Abdominal Radiology; May;41 (5):963-9.

30. **Burrel M, Llovet JM, Ayuso C, Iglesias C, Sala M, Miquel R, Caralt T, Ayuso JR, Solé M, Sanchez M, Brú C** (2003): MRI angiography is superior to helical CT for detection of HCC prior to liver transplantation: an explant correlation. Hepatology; Oct 1;38(4):1034-42.

31. **Choi JY, Lee JM, Sirlin CB** (2014): CT and MR imaging diagnosis and staging of hepatocellular carcinoma: part II. Extracellular agents, hepatobiliary agents, and ancillary imaging features. Radiology;273(1):30

32. **Ham J.H., Yu JS., Choi J.M, Cho US, Kim J H and Chung J** (2021):Corona enhancement can substitute enhancing capsule in the imaging diagnosis of small (≤ 3 cm) HCCs on gadoxetic acid–enhanced MRI. Eur Radiol: 31, 8628–8637

33. **Matsui O, Kobayashi S, Sanada J** (2011): Hepatocelluar nodules in liver cirrhosis: hemodynamic evaluation (angiography-assisted CT) with special reference to multi-step hepatocarcinogenesis. Abdom Imaging; 36(3):264–72.

34. **Granata V, Fusco R, Avallone A, Filice F, Tatangelo F, Piccirillo M, Grassi R, Izzo F, Petrillo A** (2017): Critical analysis of the major and ancillary imaging features of LI-RADS on 127 proven HCCs evaluated with functional and morphological MRI: Lights and shadows. Oncotarget; Aug 8; 8(31):51224.

35. **Rimola J, Forner A, Tremosini S, Reig M, Vilana R, Bianchi L, Rodríguez-Lope C, Solé M, Ayuso C, Bruix J** (2012): Non-invasive diagnosis of hepatocellular carcinoma 2 cm in cirrhosis. Diagnostic accuracy assessing fat, capsule and signal intensity at dynamic MRI. Journal of hepatology; Jun 1;56(6):1317-23.

36. **Forner A, Vilana R, Ayuso C, Bianchi L, Solé M, Ayuso JR, Boix L, Sala M, Varela M, Llovet JM, Brú C.** (2008): Diagnosis of hepatic nodules 20 mm or smaller in cirrhosis: prospective validation of the noninvasive diagnostic criteria for hepatocellular carcinoma. Hepatology; Jan;47(1):97-104.

37. **Elsayes KM, Kielar AZ, Elmohr MM, et al.** (2018): White paperof the Society of Abdominal Radiology hepatocellular carcinomadiagnosis disease-focused panel on LI-RADS v2018 for CT and MRI. Abdom Radiol; 43(10):2625-2642.

استخدام نظام بيانات وتقارير تصوير الكبد LI-RADS في فحوصات التصوير بالرنين المغناطيسي الديناميكية لتمييز سرطان الخلايا الكبدية عن الآفات البؤرية الكبدية الأخرى في المرضى المعرضين لخطر الإصابة بسرطان الكبد

هبه سعيد اللبان و رشا عبد الحفيظ على و سامح ابو قورة:

قسم الاشعة التشخيصية معهد الكبد القومى شبين الكوم - المنوفيه

تم إنشاء نظام بيانات وتقارير تصوير الكبد (LI-RADS) لتوحيد تصوير الكبد في المرضى المعرضين لخطر الإصابة بسرطان الخلايا الكبدية (HCC)و ساعد في تقييم الاستجابة للعلاج. حيث يعتبريوجد لسرطان الكبد (HCC) خاصًا بين الأورام الخبيثة المختلفة سمات مميزة للورم الاشعة المقطعية أو التصوير بالرنين المغناطيسي الديناميكي الذي يسمح بالتشخيص الدقيق دون اللجوء لخزعة كبدية.

الهدف: الهدف من هذه الدراسة هو تقييم العائد التشخيصي لطريقة التصوير هذه التي تم تقديمها مؤخرًا باستخدام أحدث خوارزمية LI-RADS لتمييز سرطان الخلايا الكبدية عن الآفات البؤرية الكبدية الأخرى في المرضى المعرضين لمخاطر عالية للاصابة بسرطان الكبد

الطريقة: تم جمع البيانات بأثر رجعي وتضمنت ٨٥ مريضا مصابين بآفات بؤرية حميدة وخبيثة والذين خضعوا للتصوير بالرنين المغناطيسي الديناميكي. تم إجراء التحليلات المرئية والكمية لعمليات التصوير بالرنين المغناطيسي الديناميكية. ، ارتبطت النتائج التي تم الحصول عليها بمتابعة التصوير التسلسلي للحالات أو التشخيص التشريحي المرضي كمعيار تشخيصي مرجعي

معايير التضمين هي: يتم التعرف على المريض المصاب بالعدوى الكبدية المزمنة بفيروس التهاب الكبد B و C في جميع أنحاء العالم على أنهما العوامل الرئيسية المشاركة في تسرطن الكبد.

معايير الاستبعاد هي: العلاج السابق (إما العلاج التدخلي أو الجهازي) ، ونقص قاعدة البيانات السريرية وعدم توافر المتابعة التصوير التسلسلى للحالات او التشخيص التشريحى للورم

النتائج: اشتملت الدراسة على ٨٥ مريضًا يشكون من التهاب الكبد المزمن C أو B مقسمة إلى ٥ فئات من LR1 إلى LR5 وفقًا لنظام LIRAD ، وتضمنت الميزات الإضافية لـ LIRADS

الميزات التي تفضل الأورام الخبيثة مثل شدة T2WI الخفيفة إلى المعتدلة ، درجة الانتشار ، والدهون داخل الآفة ، وتعزيز الهالة ، وتعزيز الكبسولة ، والدم داخل الآفة. كل هذه الميزات مع قيم الحساسية والخصوصية.

الميزات التي تفضل الحميدة مثل شدة T2WI العالية وتعزيز تجمع الدم مع قيم الحساسية والنوعية.

استنتاج: استخدام LI-RADS في فحوصات التصوير بالرنين المغناطيسي الديناميكية لتمييز سرطان الخلايا الكبدية عن الآفات البؤرية الكبدية الأخرى في المرضى المعرضين لمخاطر عالية لسرطان الكبد